The Journal of Pathology: Clinical Research
J Pathol Clin Res; July 2019; **5:** 154–163
Published online 25 April 2019 in Wiley Online Library (wileyonlinelibrary.com). DOI: 10.1002/cjp2.128

ORIGINAL ARTICLE

Disparate cell proliferation and p53 overexpression in colonic crypts with normal epithelial lining found below the neoplastic canopy of conventional adenomas

Carlos A Rubio[1]* and Peter T Schmidt[2]

[1]*Department of Pathology, Karolinska Institute and University Hospital, Stockholm, Sweden*
[2]*Department of Medicine, Karolinska Institute and University Hospital, Centre for Digestive Diseases, Stockholm, Sweden*

**Correspondence: Carlos A Rubio, Gastrointestinal and Liver Pathology Research Laboratory, Department of Pathology, Karolinska Institute and University Hospital, Stockholm 171 76, Sweden. E-mail: carlos.rubio@ki.se*

Abstract

We previously found colonic crypts with normal epithelial lining but with corrupted shapes (NECS) beneath the adenomatous tissue of conventional adenomas (CoAs). Here we assessed the distribution of proliferating cells (PCs) and explored the possible occurrence of p53-upregulated cells in the NECS in a cohort of CoAs. Sections from 70 CoAs and from 12 normal colon segments were immunostained with the proliferation marker Ki67. In 60 of the 70 CoAs, additional sections were immunostained for the tumor suppressor p53 protein. NECS with asymmetric, haphazardly distributed single PC or PC clusters were recorded in 80% of the CoAs, with a continuous PC domain in one or both slopes of the crypts in 17%, and with haphazardly distributed single PCs in the remaining 3% of the CoAs. In the 12 normal segments (controls), the colon crypts demonstrated normal shapes with symmetric PC domains limited to the lower third portion of the crypts. In 30% of the 60 CoAs immunostained with p53 the NECS revealed haphazardly distributed p53-upregulated cells, singly or in clusters. In sum, the apparently normal epithelium of the NECS beneath the adenomatous tissue of CoAs revealed an unprecedented relocation of the normal PC domains. This unexpected event and the occurrence of p53-upregulated cells strongly suggest that the crypts beneath the neoplastic tissue of CoAs harbor somatic mutations. The accretion of putative mutated NECS beneath the neoplastic canopy of CoA emerges as a previously unaddressed major event, an event that might play an important role in the histogenesis of CoA in the human colon.

Keywords: conventional colon adenomas; normal crypts; corrupted shapes; abnormal cell proliferation

Received 16 December 2018; Revised 18 February 2019; Accepted 25 February 2019

No conflicts of interest were declared.

Introduction

It is generally accepted that the vast majority of colonic carcinomas evolved from sporadic conventional (tubular or villous) adenomas (CoA) via the adenoma–carcinoma pathway [1–4]. In a survey of all colorectal adenomas registered at this hospital between 1993 and 2000, we found that, out of 3135 colorectal adenomas, 93% were sporadic CoAs and the remaining 7% traditional serrated adenomas (serrated and microtubular) [5]. These results substantiated the notion that sporadic CoA is the most commonly reported histologic phenotype of colorectal adenomas.

The mucosa in the normal colon is built with glands or crypts, aligned as tightly packed invaginations perpendicular to the surface epithelium, with their blind-ends 'resting' on the *muscularis mucosae* [6,7]. Despite crypts replicating by symmetric fission beginning at their base and proceeding upwards until two identical individual crypts are formed, crypt branching is seldom seen in fixed preparations from the normal colon [6,7]. Immunostaining of the colonic mucosa with the nuclear antigen Ki67, a protein marker of DNA-synthesizing epithelial cells, discloses actively proliferating cells (PCs) – cells committed to cell division – in the lower third of the crypts [8–11]. Studies in elderly patients [10] and in patients with colon carcinoma [11] revealed a significant upper expansion of the proliferative zone in the normally shaped crypts in the nonaffected colon. Based on these findings, it was

postulated that, despite neoplastic lesions being found in a restricted area, the entire colon might be predisposed to neoplastic transformation [11].

We previously found colonic crypts lined with normal epithelium, albeit with shape distortions, underneath the adenomatous glands of sporadic CoA, not only in rats [12] but also in humans [13]. These distorted crypts were referred to as crypts with normal epithelium but with corrupted shapes (NECS) [14]. In a preliminary study in six cases, we found asymmetrically, haphazardly distributed PCs in NECS below CoAs [15].

The p53 transcription factor (encoded by the human gene *TP53*) is a key tumor suppressor that regulates several signaling pathways involved in carcinogenesis. Given the resources required for *TP53* gene sequencing, most workers have used p53 immunohistochemistry as a surrogate, assuming that p53 overexpression is connected with a mutation, and that the lack of abnormal expression is indicative of WT p53. In a previous publication we found p53 upregulation in the neoplastic tissue of 25% out of 433 CoAs [16]. In that publication, NECS were not investigated.

The aim of this study was to assess the distribution of PCs and to explore possible p53 upregulation in NECS from a cohort of CoAs, the most frequent sporadic adenoma phenotype in the human colon [1–5].

Materials and methods

The material consists of sections from 85 consecutive endoscopically removed colonic conventional (tubular or villous) adenomas, without submucosal invasion. Sections were retrieved from the files of the Gastrointestinal Research Laboratory of this department.

Histological sections (4 μm thick) were stained with H&E, immunoassayed with the proliferation marker Ki67 (batch MIB1, DAKO Automation, Denmark), and with the primary mouse monoclonal antibody (IgG1, kappa, Abcam) directed against human p53 protein (antip53, DO-7; Ventana Medical System Inc., Roche, Switzerland). NECS cells exhibiting strong immune reactivity were regarded as overexpressing the p53 protein.

Recording the size of sections in CoA

Sections from CoA were reviewed using a standard Nikon light microscope, Sweden, UK, using ×10 ocular lenses and a ×2 Plan Apo objective (aperture 0.1). At that magnification, the entire field of vision (FOV) was 10 mm in diameter. CoAs contained within the boundaries but not surpassing the limits of the FOV, were regarded as small adenomas (≤10 mm), and those beyond the limits of the FOV as large adenomas (>11 mm).

Distribution of PCs in NECS

When the Ki67 antibody reacts with its cognate antigen, all transit amplifying daughter (TAD) cells become labeled [8–11,17]. Using ×10 ocular lenses and a ×4 Apo objective (aperture number 0.20), the FOV was 5 mm in diameter. At that magnification, the PC in NECS could easily be identified.

The following PC phenotypes were found in the 70 CoA: (1) haphazardly distributed single PCs, (2) haphazardly distributed PC clusters (≥2 consecutive PCs), and (3) continuous PC domain in one or in both sides of the crypts. Since the PC distribution in NECS could vary in individual CoAs, the predominant NECS PC phenotype was selected. The intense PC found in the adenomatous tissue above NECS served as internal control.

Histology of colon crypts in controls

The normal colon mucosa is built with a single epithelial cell layer exhibiting finger-like invaginations or folds, called crypts. When histological sections are cut perpendicular to the mucosal surface, the crypts appear as parallel 'row of test tubes' [6,7]. The lining epithelium is composed of mucus-secreting goblet cell and columnar absorptive cells. Goblet cells occupy practically the entire crypt, particularly in the distal colon [18].

Distribution of cell proliferation in normal colon crypts from controls

Sections from 12 grossly normal colonic segments proximal or distal to the surgically removed colonic adenocarcinoma were immunostained for Ki67. The PC distribution in the crypts was assessed using a 5 mm FOV.

Statistical analysis

The nonparametric Kruskal–Wallis test was applied, to compare difference between groups. Statistical significance was defined as $p < 0.05$.

This study was approved by The Regional Ethical Review Board in Stockholm (No. 2018/688-32).

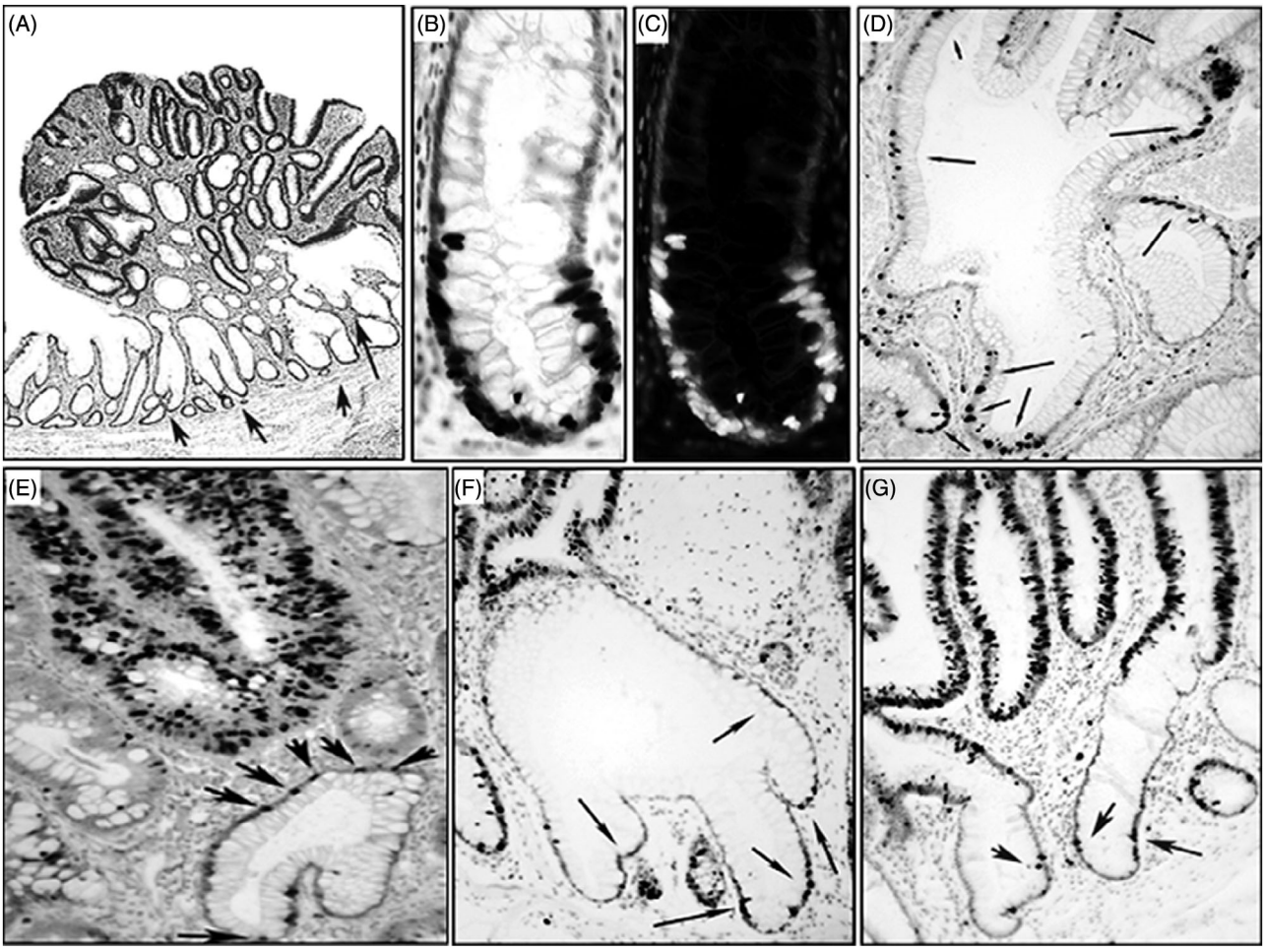

Figure 1. (A) PCs in crypts with normal epithelium but with corrupted shapes (NECS, at arrows), found underneath the adenomatous epithelium of a CoA (H&E, original ×1). (B) PCs in a normal colon crypt. Note PCs symmetrically aligned in 'Indian files' along both slopes of the lower third of the crypt (control, Ki67, batch MIB1, original ×40). (C) The same as (B), after applying the Invert Function within ADOBE PHOTOSHOP CS6 (Ki67, original ×40). (D) Multilobate NECS showing asymmetric distribution of PCs in the normal epithelial lining (Ki67, batch MIB1, original ×10). (E) NECS showing continuous PCs, at arrows. Note intense cell proliferation in the adenomatous tissue on top (Ki67, batch MIB1, original ×4). (F) Multilobate NECS showing asymmetric PC distribution in the normal epithelial lining (Ki67, batch MIB1, original ×20, at arrows). (G) NECS showing asymmetric distribution of PCs in the normal epithelial lining, at arrows. Note intense cell proliferation in the adenomatous tissue on top (Ki67, batch MIB1, original ×20).

Results

A total of 10 out of the 85 CoAs were rejected from the study since the full length of the crypts had been totally replaced by the adenomatous epithelium. In addition, five CoAs were also rejected from the study because of poorly orientated, tangentially cut sections. Thus, the present study includes 70 CoAs immunostained for Ki67. Preliminary results of PC in NECS from 6 of the 70 CoA reported here were published elsewhere [15]. In 60 of the 70 CoAs, additional sections were immunostained for the tumor-suppressor p53 protein.

Frequency of NECS in small and large CoA

Using ×10 ocular lenses and a ×2 Plan Apo objective (FOV = 10 mm) showed that 12 of the 70 CoAs measured ≤10 mm (mean 8.4 mm, range 7–10 mm), and the remaining 58 CoAs measured >11 mm (mean 16.1 mm, range 12–23 mm). The number of NECS in the 12 small CoA was 184 (mean 19.3, range 6–30), and the number of NECS in 14 unselected large CoAs was 267 (mean 20.1, range 8–25). The differences in the frequency of NECS between small and large CoAs was nonsignificant ($p = 0.12$).

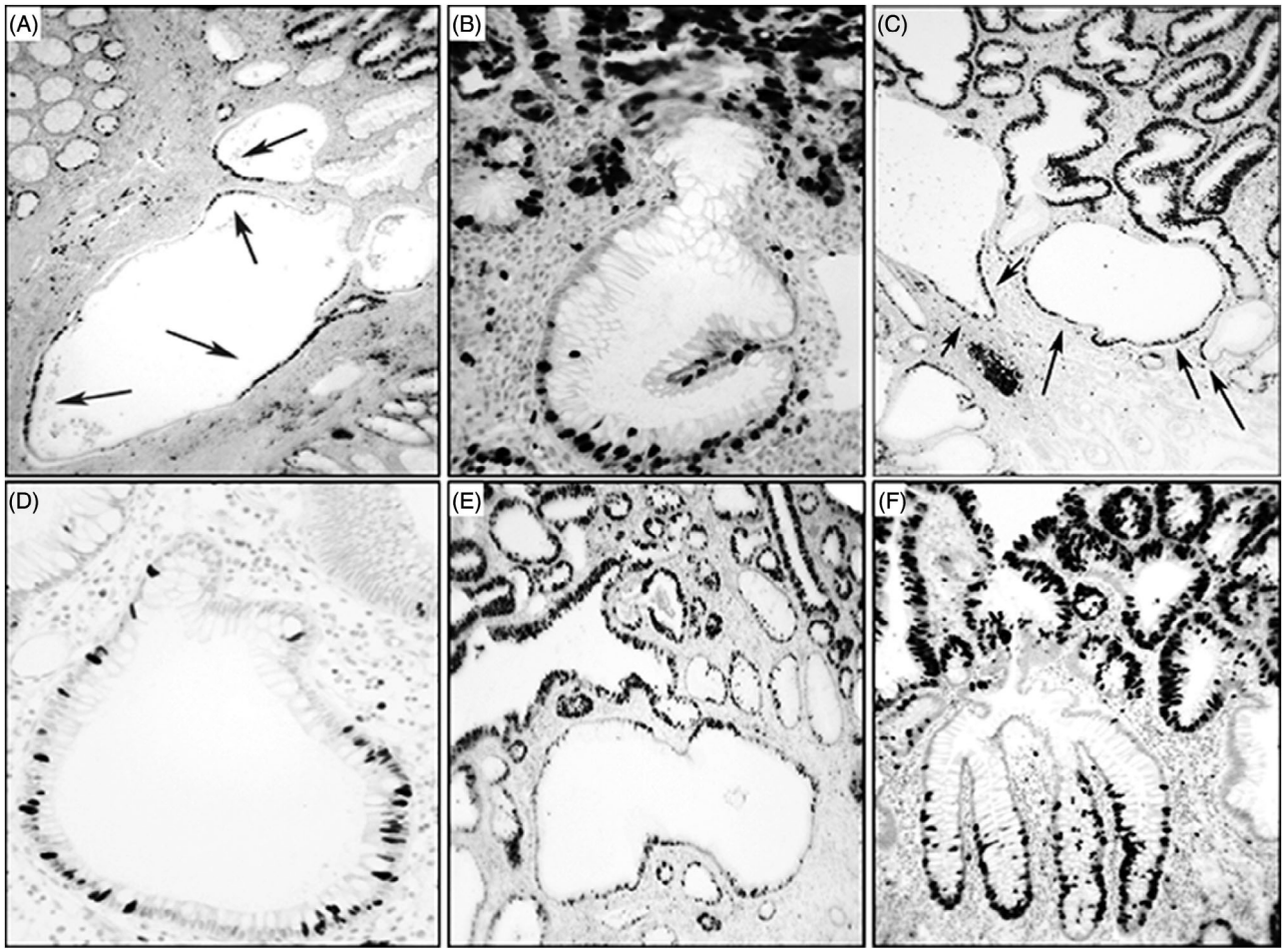

Figure 2. (A) Cystically dilated NECS below the adenomatous tissue in a CoA showing asymmetrically distributed PC clusters at arrows (Ki67, batch MIB1, original ×10). (B) NECS with abnormal PC-domain at its base (Ki67, batch MIB1 ×20). (C–E) More examples of cystically dilated NECS showing various asymmetrically located PC-domains in the normal epithelium. In (E), note intense cell proliferation in the adenomatous tissue on top (Ki67, batch MIB1, C and E: original ×10, D: original ×20). F: Multi-fission in a NECS displaying asymmetric PC. Note intense cell proliferation in the adenomatous tissue on top (Ki67, batch MIB1×10).

Distribution of PC in NECS below CoA

Qualitative examination disclosed an abnormal distribution of PC-domains in the NECS in all 70 CoA (Figures 1–3). Quantitative examination – using 5 mm FOV – revealed a total of 1230 NECS (mean 17.5, range 6–30) below the 70 CoAs.

The frequency of predominant PC phenotypes in NECS from the 70 CoA is shown in Table 1. It is seen that NECS with haphazardly distributed PC clusters were present in 80% of the CoAs, with continuous PC in one or both slopes of the crypts in 17% of the CoAs, and with haphazardly distributed single PCs in the remaining 3% of the CoA. The difference between CoA with NECS exhibiting haphazardly distributed PC clusters and the other two groups in Table 1 was significant ($p < 0.05$).

Distribution of PCs in controls

Immunostained sections were studied within a 5 mm FOV in the 12 control cases. A total of 692 normal crypts (mean 57.6/control segment, range 52–68) were found in the 12 control specimens. All 692 normal crypts showed symmetrically aligned PCs in uninterrupted 'Indian files' along both slopes of the lower third of the crypts (Figure 1B,C).

p53 upregulation in NECS below CoA

Table 2 shows that, in the neoplastic tissue, p53 was overexpressed in 33% out of the 60 CoAs. This percentage was similar to that found in a previous survey at this department, where 25% out of the 433 CoAs exhibited p53 overexpression in the neoplastic tissue

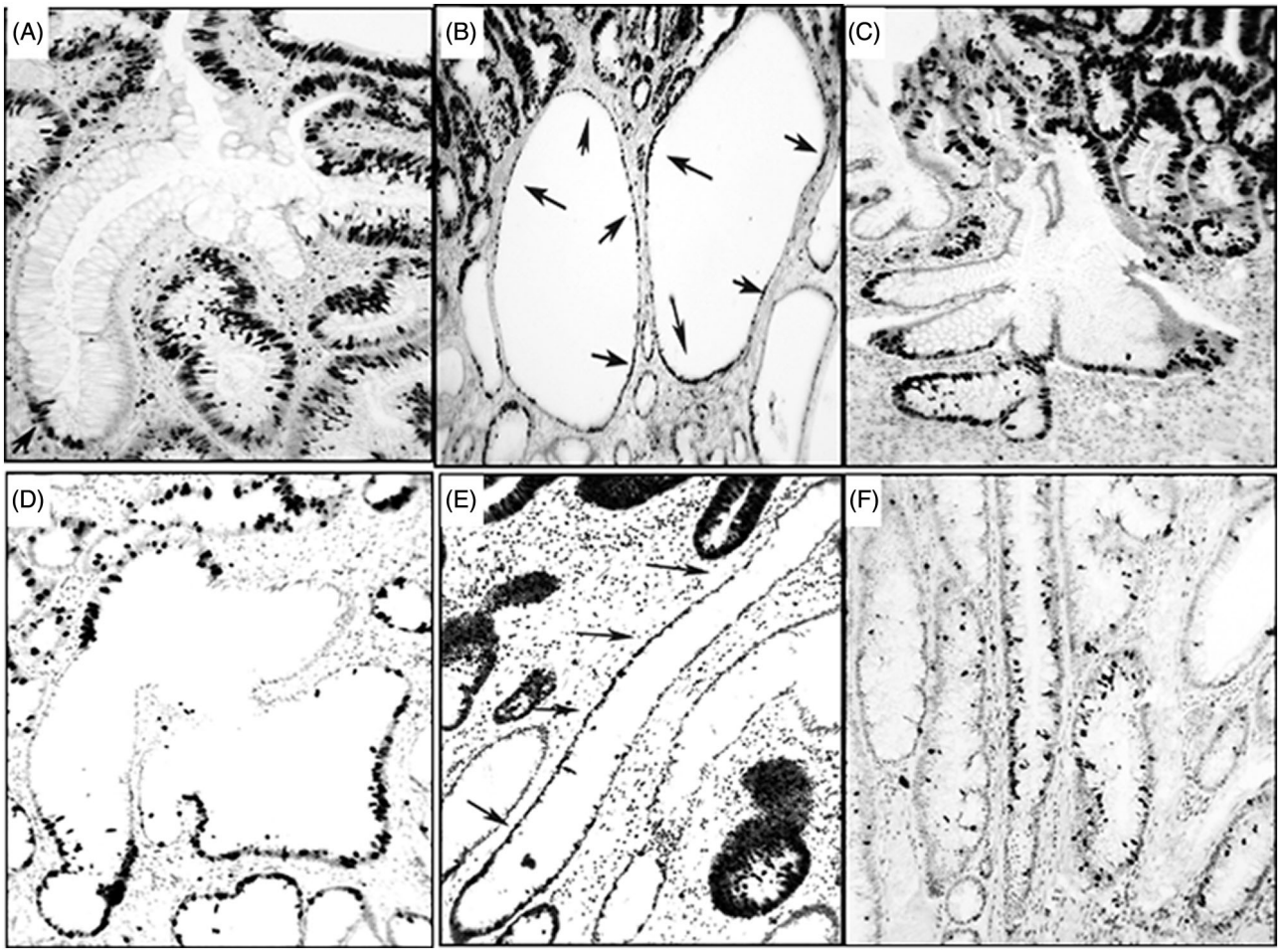

Figure 3. (A–F) More examples of NECS found underneath the adenomatous tissue of CoAs showing asymmetric clusters of cell proliferation. (A,D) Original ×20, (B,C,E,F): original ×10 (Ki67, batch MIB1). In E, note continuous PCs in the left slope of an hyperplastic NECS, and, in F, note continuous PCs in the both slopes of an hyperplastic NECS.

Table 1. The predominant PC phenotype found in crypts with NECS found below the adenomatous tissue of 70 CoAs

Predominant PC phenotypes in NECS	CoA, *n* (%)
Asymetric, haphazardly distributed PC clusters	50 (80)
Continuous PC in one or in both sides of the crypts	12 (17.1)
Haphazardly distributed single PC	2 (2.9)
All	70 (100)

The predominant PC phenotype in NECS was chosen to represent each CoA. PC clusters: those showing ≥2 contiguous labeled cells.

Table 2. p53 overexpression in the neoplastic tissue and in the crypts with NECS found below the neoplastic tissue in 60 CoAs of the colon

p53	Overexpression (+)	No expression (–)	All CoA
Neoplastic tissue in CoA	20 (33%)	40 (67%)	60 (100%)
NECS	18 (30%)	42 (70%)	60 (100%)

[16]. The same table reveals that, below the neoplastic tissue, p53 was overexpressed in the NECS of 30% of the 60 CoAs. In the remaining 70% of the CoAs, all NECS cells were unstained following p53 immunostaining.

Table 3. Age, localization and p53 upregulation in crypts with NECS below the neoplastic epithelium in 60 CoAs of the colon

	NECS overexpressing p53 *n* = 18 (%)	CoA cases immuno-stained with p53 *n* = 60 (%)
Age		
≤59 years	7 (39)	25 (42)
≥60 years	11 (61)	35 (58)
Localization*		
Right colon	8 (44)	22 (37)
Left colon	10 (56)	38 (63)

*Right colon: colon proximal to the splenic flexure and left colon: colon distal to the splenic flexure.

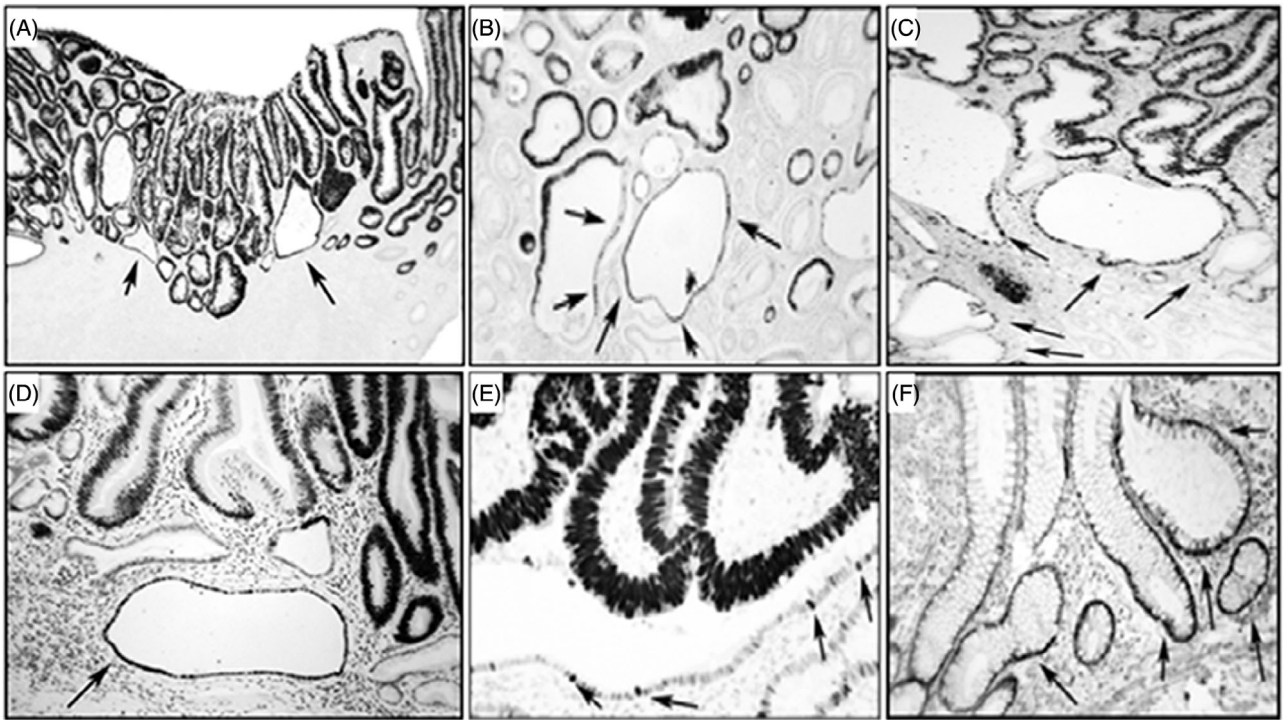

Figure 4. (A) p53-overexpression in crypts with NECS found underneath the neoplastic epithelium of a conventional colon adenoma (CoA). Note intense p53 upregulation in the neoplastic epithelium on top of NECS with p53-upregulated clusters at arrows (p53 immunostain, original ×4). (B–D) Cystically dilated NECS underneath the adenomatous tissue of a CoA, exhibiting p53-upregulated cell clusters at arrows (p53 immunostain, original ×10). (E) Closer view of NECS exhibiting single cell p53 upregulation, at arrow. Note exstensive p53 upregulation in the neoplastic tissue of the CoA on top (p53 immunostain, original ×40). (F) p53 overexpression in hyperplastic and cystic NECS phenotypes found below the adenomatous epithelium of a CoA (p53 immunostain, original ×20).

Table 3 shows no essential differences between the age of the patients, the localization of the NECS and p53 upregulation.

Discussion

This study demonstrates that NECS coexist with haphazardly distributed PCs, often in asymmetric clusters. These findings are at variance with those in the crypts from normal controls, where continuous labeled cells are symmetrically aligned lengthwise in the lower third of the crypts.

In the normal colon the stem cells are located at the base of crypts; those stem cells synchronize the repopulation of the crypts by generating progenitor cells, called TAD cells [17,19]. Progenitor cells (120–150 TAD cells/crypt according to Testa *et al* [20]) account for the bulk of the PCs in the crypts. Since the PC domain is generated by stem cells in normal crypts [19,20], the occurrence of multiple PC clusters in TAD cells from NECS rationally implies that several stem cells/NECS do exist. This deduction appears to be in concert with studies in humans by Baker *et al* [21], showing that 5–6 stem cells exist in each normal colon crypt. However, at variance with the natural position of the stem cells at the base of normal crypts [8–11,19–22], the stem cells in NECS appear to have been relocated. It should be stressed that, in some NECS, more than 10 PC domains were found (Figure 2D) suggesting that the additional stem cells might be migrant stem cells of bone marrow origin [23].The displacement of the normal position of the PCs in NECS, often as asymmetrically distributed PC clusters, and less commonly as haphazardly distributed single cells, supports earlier claims that the normal-looking epithelium in NECS might have been subjected to somatic mutations [13]. These considerations are substantiated by the present results showing that p53 was upregulated in NECS, either in single cells or in cell clusters (Figures 4 and 5).

Goodblad *et al* [24] showed that there are up to 15 times more mitotic figures in a whole colonic

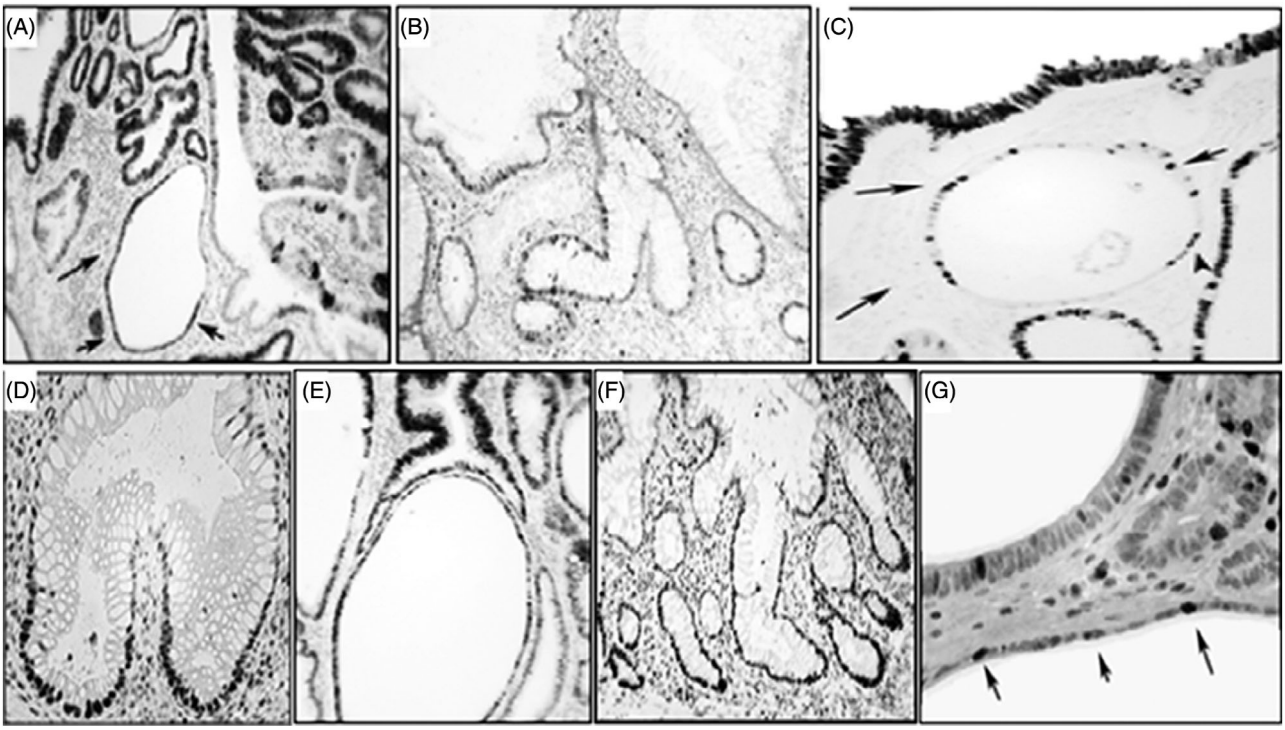

Figure 5. (A–G) More examples of p53-overexpression in crypts with NECS, found below the neoplastic epithelium of conventional colon adenoma (CoA). Note NECS with p53-upregulated clusters (p53 immunostain, A: original ×4. B: original ×10, C: original ×20, D: original ×10, E: original ×20, F: Closer view of a NECS showing p53 upregulation in single cells, at arrows (original ×10, G original ×40).

crypt than in the 4 μm-thick histological sections that were used in their studies. Since the number of PCs/crypt is much higher than the number of mitotic cells/crypt [24], the possibility that NECS with multiple single PCs, or with one or more PC clusters, could contain a much higher number of DNA-synthesizing cells elsewhere in other areas from the same crypt, cannot be rejected. It should be stressed that, in present study, we also used 4 μm-thick sections to assess PCs.

Boman and Fields asserted that normal crypts began to show abnormalities in histology only when they became dysplastic [25]. The present demonstration that NECS below the adenomatous canopy of CoA contained haphazardly distributed, often asymmetric, PC clusters strongly suggests that, in addition to morphological (H&E) changes [13], profound biological alterations in the regulation of cell proliferation also ensue in NECS.

The question is whether the various PC phenotypes found in NECS after fixation are permanent over time or erratic at any given time of observation. If the latter is the case, then the putative relocation of the stem cells in NECS emerges as a novel challenging alternative in the natural evolution of CoA. The haphazard distribution of PCs, and the putative relocation of stem cells in NECS, also raises the question as to whether the relatively stable equilibrium between interdependent elements orchestrating stem cell-crypt homeostasis, has been severely altered in NECS.

The finding that the number of NECS/10 mm FOV was significantly lower than in controls indicates that the width of the crypts is an essential parameter in distinguishing between NECS and normal crypts. Considering that human colonic crypts typically divide at most once or twice during a lifetime, with an average crypt cycle length of 36 years [21], the accretion of NECS with PC anomalies beneath conventional adenomas (CoAs) emerges as a remarkable finding.

None of the colonic crypts in controls displayed NECS, thereby substantiating descriptions of the normal colonic mucosa in the literature [7,10,11]. The crucial question is: what are the morphogenic mechanisms that induce colonic crypts, lined with normal epithelium, to assume corrupted shapes beneath CoA? Morphogenesis stands for the ability of a system to change its form [26]. Jagan *et al* demonstrated that the formation of colorectal crypts is regulated by phosphatase and tensin homolog (PTEN), a protein encoded by the *PTEN* gene [26] . In addition, Georgescu *et al* [27]

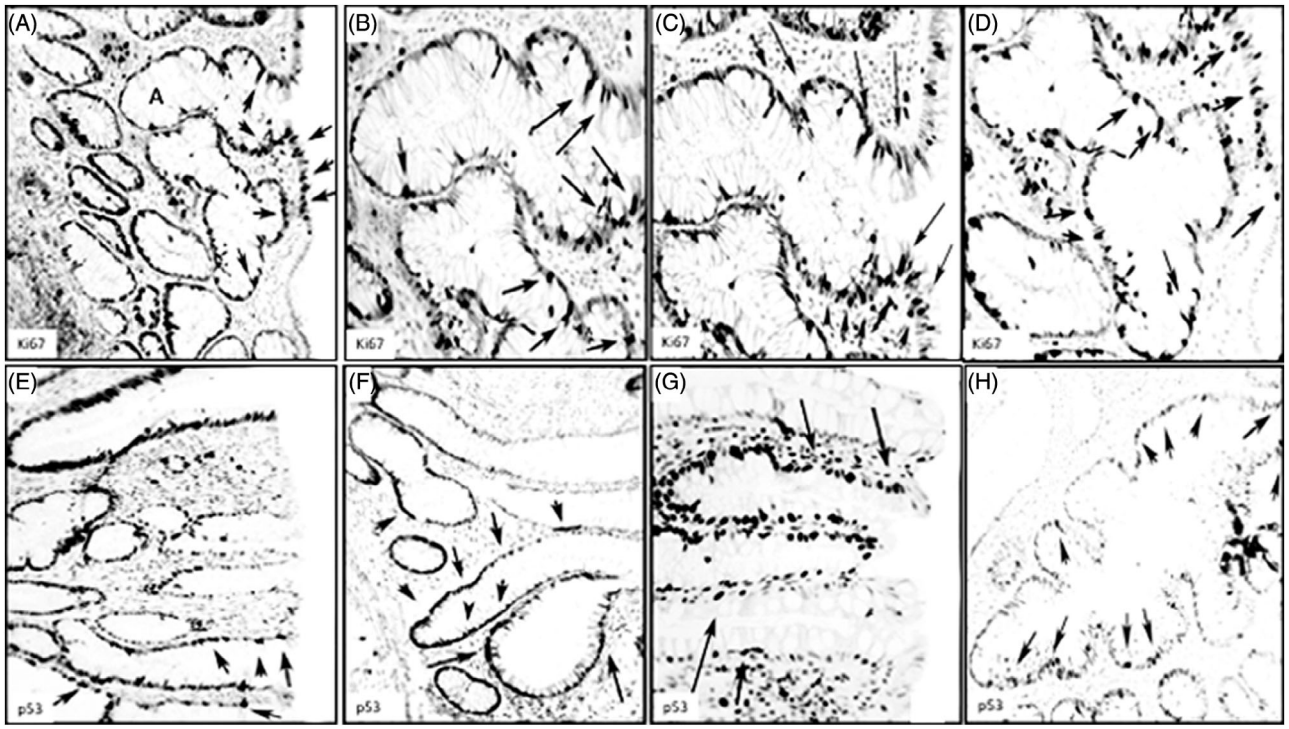

Figure 6. Crypts with NECS, found in the stalk of CoA, not covered by neoplastic epithelium. Upper panel: Ki67 immunostaining, (A) asymetric, haphazardly distributed PCs in the superficial aspect of crypts with NECS (at arrows), found in the stalk of CoA, not covered by neoplastic epithelium (Ki67, batch MIB1, ×10). (B) and (C) closer views of (A) in (A) showing haphazardly distributed PCs in the superficial and deeper aspects of NECS (at arrows) found in the stalk of CoA, not covered by neoplastic epithelium (Ki67, batch MIB1, ×20). (D) Another close view showing atypical PC distribution reaching the superficial aspect of NECS in the stalk (at arrows) Ki67, batch MIB1, ×20). Lower panel: p53 immunostaining, (E–H) Upregulated p53 cells found in NECS (at arrows) in the stalk of CoA, not covered by neoplastic epithelium (p53 immunostain, E–H: original ×10).

found in three-dimensional studies of human colon glands that NHERF1 protein, a Na^+/H^+ exchanger regulatory factor, controls gland morphogenesis. Thus, the NECS-phenotype might have been generated by alterations in morphogenesis signals such as NHERF1 and PTEN.

Surprisingly, 30% of the NECS below the neoplastic canopy of CoA showed haphazardly distributed p53-upregulated cells, suggesting putative mutations. In some CoA, the p53 overexpression was found in cystically dilated NECS (Figures 4 and 5). In this context, we previously studied the occurrence of nonneoplastic glandular cysts beneath gastric adenomas [28]. Micrometric assessment showed that the subjacent cysts were larger beneath the neoplastic tissue than in the adjacent nonneoplastic gastric mucosa. In some glands, clusters of dysplastic cells were found at the narrowest part of the outlet from the glands, substantiating an obstructive-causal mechanism [28]. A similar mechanism might apply to the evolution of some – but not all – NECS beneath CoA (Figures 1–5).

There is much discussion regarding the role played by stem cells in the morphogenesis of conventional colonic adenomas [29,30]. It is generally accepted that the epithelial stem cells – custodians of cell proliferation and crypt-cell renewal – reside at the base of normal crypts. The incongruity is why, in the early stages of adenomagenesis, the dysplastic cells are found at the luminal surface of the crypt orifices, while 'the bases of these same crypts appear morphologically normal' [29]. To explore that conundrum, the Vogelstein group [29] evaluated the molecular characteristics of cells isolated from the bases and orifices of the same crypts. It was found that the dysplastic cells at the tops of the crypts often exhibited genetic alterations of adenomatous polyposis coli and neoplasia-associated patterns of gene expression. In contrast, the cells at the base of these same crypts did not contain such alterations. It was deduced that the mutant cells in the zone between crypt orifices expanded, migrating laterally and downwards to displace the normal epithelium of adjacent crypts in a 'top-down' manner [29].

An opposite view was propounded by the Wright group [30]. Based on the finding of unicryptal (monocryptal) colon adenomas in patients with familial adenomatous polyposis, the authors proposed a 'bottom-up' replacement trail for the histogenesis of colon adenomas. It was assumed that the mutated clone in monocryptal adenomas expanded by symmetrical crypt fission, usually at the base, or by crypt budding, following a 'bottom-up pattern'. However, since monocryptal adenomas are extremely rare in sporadic cases, it was finally concluded that a 'top-down pattern' prevailed in sporadic adenomas [30].

Based on the present findings, we have envisaged an alternative view. While studying the mucosa of the stalk in CoA, we found NECS without adenomatous tissue on top. Some of these NECS in the stalk showed haphazardly distributed single PC or PC clusters (Figure 6A–D) and p53-upregulated cells (Figure 6E–H), strongly suggesting that NECS might undergo mutations without the participation of neoplastic tissue on top. The finding of superficial PC at the level of the crypt orifices, and considering that no PCs exist without the support of a stem cell, it is hypothesized that, triggered by the alleged mutagenic microbiota of the fecal microenvironment [31–35], the superficial mutated stem cells might have undergone a series of further mutations leading to dysplastic changes. In contrast, deeper stem cells would remain 'protected' by the microenvironment of the stem cell niche and of the stromal niche [36]. Eventually, superficial dysplastic PCs in CoA (Figure 6), would replace the normal-looking epithelium of the NECS in a 'top-down' manner.

In sum, an unprecedented reorganization of PC domains and of p53-upregulated cells ensue in the normal epithelium of the NECS found beneath the neoplastic tissue of CoA. These unexpected events strongly suggest that the crypts with corrupted shapes beneath the neoplastic tissue of CoA harbor somatic mutations. The accretion of putative mutated NECS beneath the neoplastic canopy of CoA emerges as a previously unaddressed major event, an event that might play an important role in the histogenesis of CoA in the human colon.

Author contributions statement

CAR designed the experiment, performed procedures, data analysis, and wrote the manuscript. PTS harvested all adenomas endoscopically, introduced suggestions, and approved the final manuscript.

References

1. Jackman RJ, Mayo CW. The adenoma–carcinoma sequence in cancer of the colon. *Surg Gynecol Obstet* 1951; **93:** 327–330.
2. Winawer SJ, O'Brien MJ, Waye JD, *et al*. Risk and surveillance of individuals with colorectal polyps. WHO collaborating centre for the prevention of colorectal cancer. *Bull World Health Organ* 1990; **68:** 789–795.
3. Calderwood AH, Lasser K, Roy H. Colon adenoma features and their impact on risk of future advanced adenomas and colorectal cancer. *World J Gastrointest Oncol* 2016; **8:** 826–834.
4. Forsberg A, Kjellström L, Andreasson A, *et al*. Colonoscopy findings in high-risk individuals compared to an average-risk control population. *Scand J Gastroenterol* 2015; **50:** 866–874.
5. Rubio CA. Colorectal adenomas: time for reappraisal. *Pathol Res Pract* 2002; **198:** 615–620.
6. Levine DS, Haggitt RC. Normal histology of the colon. *Amer J Surg Pathol* 1989; **3:** 966–984.
7. Rubio CA. The histologic structure of the large bowel mucosa and the evolution of the three pathways of colonic carcinogenesis in humans and in experimental animals. In: *Recent Studies on Digestive System Anatomy*, Volume **3**, 2018; 1–12. http://openaccessebooks.com/digestive-system-anatomy.html.
8. Deschner EE. Cell proliferation and colonic neoplasia. *Scand J Gastroenterol Suppl* 1988; **151:** 94–97.
9. Humphries A, Wright NA. Colonic crypt organization and tumorigenesis. *Nat Rev Cancer* 2008; **8:** 415–424.
10. Paganelli GM, Santucci R, Biasco G, *et al*. Effect of sex and age on rectal cell renewal in humans. *Cancer Lett* 1990; **53:** 117–120.
11. Ponz de Leon M, Roncucci L, Di Donato P, *et al*. Pattern of epithelial cell proliferation in colorectal mucosa of normal subjects and of patients with adenomatous polyps or cancer of the large bowel. *Cancer Res* 1988; **48:** 4121–4126.
12. Rubio CA. Corrupted colonic crypt fission in carcinogen-treated rats. *PLoS One* 2017; **12:** e0172824.
13. Rubio CA, Schmidt PT. Are non-dysplastic crypts with corrupted shapes the initial recordable histological event in the development of sporadic conventional adenomas? *Anticancer Res* 2018; **38:** 3811–3815.
14. Rubio CA, Schmidt PT. Morphological classification of corrupted colonic crypts in ulcerative colitis. *Anticancer Res* 2018; **38:** 2253–2259.
15. Rubio CA. Multiple clusters of cell proliferation in non-dysplastic corrupted colonic crypts underneath conventional cdenomas. *In Vivo* 2018; **32:** 1473–1475.
16. Rubio CA, Rodesjö M, Duvander A, *et al*. p53 up-regulation during colorectal carcinogenesis. *Anticancer Res* 2014; **34:** 6973–6979.
17. Rubio CA. Chapter 10: Putative stem cells in mucosas of the esophago-gastrointestinal tract. In: *Stem cell, regenerative medicine and cancer*Singh SR (Ed). Nova Science Publishers Inc.: New York, 2010; 279–308.
18. Mello Rde O, Silva CM, Fonte FP, *et al*. Evaluation of the number of goblet cells in crypts of the colonic mucosa with and without fecal transit. *Rev Col Bras Cir* 2012; **39:** 139–145.

19. Davies PS, Dismuke AD, Powell AE, *et al*. Wnt-reporter expression pattern in the mouse intestine during homeostasis. *BMC Gastroenterol* 2008; **8:** 57–62.
20. Testa U, Pelosi E, Castelli G. Colorectal cancer: genetic abnormalities, tumor progression, tumor heterogeneity, clonal evolution and tumor-initiating cells. *Med Sci* 2018; **6:** 31–46.
21. Baker AM, Cereser B, Melton S, *et al*. Quantification of crypt and stem cell evolution in the normal and neoplastic human colon. *Cell Rep* 2014; **8:** 940–947.
22. Singh P, O'Connell M, Shubhashish S. Epigenetic regulation of human *DCLK-1* gene during colon-carcinogenesis: clinical and mechanistic implications. *Stem Cell Investig* 2016; **3:** 51–62.
23. Fu J, Zuber J, Martinez M, *et al*. Human intestinal allografts contain functioinal hematopoietic stem and progenitor cells that are maintained by a circulating pool. *Cell Stem Cell* 2019; **24:** 227–239.
24. Goodlad RA, Lee CY, Wright NA. Cell proliferation in the small intestine and colon of intravenously fed rats: effects of urogastrone-epidermal growth factor. *Cell Prolif* 1992; **25:** 393–404.
25. Boman BM, Fields JZ. An APC:WNT counter-current-like mechanism regulates cell division along the human colonic crypt axis: a mechanism that explains how APC mutations induce proliferative abnormalities that drive colon cancer development. *Front Oncol* 2013; **3:** 244–250.
26. Jagan IC, Deevi RK, Fatehullah A, *et al*. PTEN phosphatase-independent maintenance of glandular morphology in a predictive colorectal cancer model system. *Neoplasia* 2013; **15:** 1218–1230.
27. Georgescu MM, Cote G, Agarwal NK, *et al*. NHERF1/EBP50 controls morphogenesis of 3D colonic glands by stabilizing PTEN and ezrin-radixin-moesin proteins at the apical membrane. *Neoplasia* 2014; **16:** 365–374.
28. Rubio CA, Kato Y, Sugano H, *et al*. The intramucosal cysts of the stomach. VII: a pathway of gastric carcinogenesis? *J Surg Oncol* 1986; **32:** 214–219.
29. Shih IM, Wang TL, Traverso G, *et al*. Top-down morphogenesis of colorectal tumors. *Proc Natl Acad Sci U S A* 2001; **98:** 2640–2645.
30. Preston SL, Wong WM, Chan AO, *et al*. Bottom-up histogenesis of colorectal adenomas: origin in the monocryptal adenoma and initial expansion by crypt fission. *Cancer Res* 2003; **63:** 3819–3825.
31. Ene IV, Farrer RA, Hirakawa MP, *et al*. Global analysis of mutations driving microevolution of a heterozygous diploid fungal pathogen. *Proc Natl Acad Sci U S A* 2018; **115:** E8688–E8697.
32. Burns MB, Montassier E, Abrahante J, *et al*. Colorectal cancer mutational profiles correlate with defined microbial communities in the tumor microenvironment. *PLoS Genet* 2018; **14:** e1007376.
33. Mandal P. Molecular mechanistic pathway of colorectal carcinogenesis associated with intestinal microbiota. *Anaerobe* 2018; **49:** 63–70.
34. Wang X, Yang Y, Huycke MM. Microbiome-driven carcinogenesis in colorectal cancer: Models and mechanisms. *Free Radic Biol Med* 2017; **105:** 3–15.
35. Zackular JP, Baxter NT, Chen GY, *et al*. Manipulation of the gut microbiota reveals role in colon tumorigenesis. *mSphere* 2015; **1:** e00001-15.
36. Roberts KJ, Kershner AM, Beachy PA. The stromal niche for epithelial stem cells: a template for regeneration and a brake on malignancy. *Cancer Cell* 2017; **32:** 404–410.